

THE STRUCTURE AND STAR FORMATION HISTORY OF EARLY-TYPE GALAXIES IN THE UDF/GRAPES SURVEY

A. Pasquali¹, I. Ferreras², N. Panagia³, E. Daddi⁴, S. Malhotra³, J. E. Rhoads³, N. Pirzkal³, R. A. Windhorst⁵,
A. Koekemoer³, L. Moustakas³, C. Xu³, C. Gronwall⁶

Submitted to ApJ

ABSTRACT

We present a two-pronged approach to the formation of early-type galaxies, using a sample of 18 galaxies at $0.5 < z < 1$ from the HST/ACS Ultra Deep Field and GRAPES surveys: 1) We combine slitless low resolution spectroscopy from the GRAPES dataset with simple models of galaxy formation to explore their star formation histories. 2) We also perform an analysis of their surface brightness distribution with the unprecedented details provided by the ACS superb angular resolution and photometric depth. Our spectroscopic analysis reveals that their stellar populations are rather homogeneous in age and metallicity and formed at redshifts $z_F = 2-5$. Evolving them passively, they become practically indistinguishable from ellipticals at $z = 0$. Also, their isophotal shapes appear very similar to those observed for nearby ellipticals, in that the percentages of disky and boxy galaxies at $z = 1$ are close to the values measured at $z = 0$. Moreover, we find that the isophotal structure of $z = 1$ early-type galaxies obeys the correlations already observed among nearby ellipticals, i.e. disky ellipticals have generally higher characteristic ellipticities, and boxy ellipticals have larger half-light radii and are brighter in the restframe B band. In this respect then, no significant structural differences are seen for ellipticals between $z = 0$ and 1. Exception can be possibly made for the a_3/a parameter, which is larger at $z = 1$ than usually measured at $z = 0$. The a_3/a parameter measures the deviations from a pure elliptical isophote which are not symmetric with respect to the galaxy center, as in the case of dust lanes and most notably of clumps. Blue clumps have been detected in nearly 50% of the $z = 1$ early-type galaxies; their photometry is suggestive of young star clusters or dwarf irregulars if they are assumed to be at the same redshift as their host galaxies. We speculate that these clumps may represent recent accretion episodes, and that they could be a way to produce blue cores if their dynamical time is such for them to rapidly sink to the galaxy center.

Subject headings: galaxies: elliptical and lenticular, cD { galaxies: evolution { galaxies: formation { galaxies: stellar content

1. introduction

Understanding how and when galaxies formed is one of the most outstanding challenges of modern astrophysics. The traditional approach is to study their stellar populations via spectro-photometric observables (see e.g. Worthey 1994; Trager et al. 2000; Bernardi et al. 2003), derive the age and metallicity distribution of their (unresolved) stellar content and finally reconstruct their star-formation history. This is the ultimate ingredient in distinguishing between different mechanisms for the formation of ellipticals, such as monolithic collapse (Eggen, Lynden-Bell & Sandage 1962) and hierarchical merging (Kauffmann et al. 1993). Massive elliptical galaxies are the best probes for a comparison with these models, since they are dominated by old, passively evolving stellar populations (see e.g. Stanford, Eisenhardt & Dickinson 1998), whose abundance ratios imply that star formation took place over a very short period of time, possibly

shorter than 1 Gyr (see e.g. Thomas, Greggio & Bender 1999). On the other hand, the spheroidal morphology and hot dynamics observed in these systems require major mergers, which results in a more extended dynamical history. Indeed, semi-analytical models of galaxy formation { which consistently track the hierarchical merging of the underlying halos { predict a rather extended assembly history (Kauffmann & Charlot 1998) which { naively coupled to simple models of star formation { lead to wrong predictions about the abundance ratios of giant ellipticals. This apparent discrepancy can be overcome if the starburst ignited by the major merger which forms the elliptical galaxy is characterized by a significantly attenuated IMF with respect to Salpeter. This constraint is indeed able to reproduce a Mg/Fe overabundance in the stellar population of the elliptical (Thomas 1999). Hence, a combined analysis of the stellar populations in these galaxies and their detailed morphology is a powerful tool to determine the connection between mass assembly and star formation. So far, local samples of early-type galaxies have been explored, most notably those from the SAURON collaboration (de Zeeuw et al. 2002), who uses a dedicated Integral Field Unit to extract both the kinematics and the age/metallicity distribution (via Lick indices). This ongoing project has revealed the presence of interesting kinematic peculiarities { such as decoupled cores { in galaxies which do not show any structure when viewed through observables sensitive to

¹ Institut für Astronomie, HPP, ETH, 8093 Zurich, Switzerland, pasquali@phys.ethz.ch

² Department of Physics and Astronomy, University College London, Gower St. London WC1E 6BT, England

³ ST ScI, 3700 San Martin Drive, Baltimore, MD 21218, USA

⁴ Spitzer Fellow, NOAO, P.O. Box 26732, Tucson, AZ 85726, USA

⁵ Department of Physics & Astronomy, Arizona State University, P.O. Box 871504, Tempe, AZ 85287-1504, USA

⁶ Department of Astronomy, Pennsylvania State University, 525 Davey Laboratory, University Park, PA 16802

stellar ages and metallicities (Davies et al. 2001). Extending such a study to moderate redshift ($z < 1$) will set much stronger constraints on the formation process of ellipticals. Current instrumentation is not sensitive enough to probe the detailed dynamics of moderate redshift galaxies via resolved spectroscopy \a la SAURON". However, the superb spatial resolution of HST allows us to explore the 2D surface brightness distribution and to use morphology as a proxy for their dynamical state.

The advent of wide-field imaging surveys performed from the ground and with HST (e.g. Williams et al. 1996, Giallisco et al. 2004, Beckwith et al. 2005) has proved that galaxy structure evolves with time, so that more distant galaxies are more peculiar than those in the local Universe on which the Hubble classification was originally based (Driver et al. 1995, Gazebrook et al. 1995, Abraham et al. 1996, Driver et al. 1998, Brichmann & Ellis 2000, Conselice et al. 2004). Furthermore, the morphology-density relation (Dressler 1980, Dressler et al. 1997) confirms that galaxy morphology depends strongly on environment, with early-type galaxies preferentially living in high density regions. Notice, here, that the morphological K-correction can affect the morphological classification, especially depending on the fading of the surface brightness with wavelength. Windhorst et al. (2002, cf. also Colley et al. 1996) showed that early-type galaxies endure a significant decrease in their surface brightness from red to mid-UV wavelengths which could lead to a different classification and makes them almost undetectable at intermediate to high redshifts. Mid-type and star-forming galaxies appear in the mid-UV with a somewhat later type, while the majority of late-type and merging systems have a morphology little dependent on wavelength.

Galaxy shapes can be quantified into several \morphological parameters" (e.g. surface brightness profile, bulge-to-disk ratio, ellipticity, light concentration, asymmetry and clumpiness) which turn out to correlate with the galaxy star-formation rate, stellar mass, central black hole mass and merging history. For example, the light concentration of a galaxy varies with its luminosity, stellar mass, size and the mass of the central black hole (Caon et al. 1993, Graham et al. 1996, Bershadsky et al. 2000, Graham et al. 2001, Conselice 2003). Therefore, it depends on the past formation history of a galaxy. A symmetry and clumpiness \measure" a more recent epoch in the evolution of a galaxy, since asymmetry is due to the presence of a merger and/or to tidal interactions, and clumpiness correlates with the degree of on-going star formation (Conselice 2003). These correlations allow us to decipher galaxy morphologies into mechanisms of galaxy formation and into time evolution of galaxy assembly.

Extensive imaging from the ground and with HST has revealed that a large fraction of nearby elliptical galaxies (Es) differ from a pure ellipse shape and do show substructures. For example, the ellipticity is not always constant with distance from the galaxy center. DiTullio (1978, 1979) found that isolated Es are, on average, characterized by a decreasing ellipticity, while the mean ellipticity profile is either increasing or peaking with radius in Es located in galaxy clusters and groups. A change in the position angle of the galaxy major axis is often ob-

served and explained as a projection effect of a triaxial structure whose axes ratios (b/a and c/a) vary with radius (Galletta 1980, Franx 1988). About 60% of Es have \non-elliptical" isophotes, equally separated into disk or boxy (Bender et al. 1988, 1989). Disky Es are generally oblate rotators, while boxy Es span a variety of kinematical properties and are systematically bigger and brighter, suggesting that they formed via mergers (Naab, Burkert & Hemquist 1999). Almost half of the nearby Es, especially those in galaxy groups, show dust lanes which are aligned with the major or minor axis and thus believed to be byproducts of mergers (Lauer 1985, Sadler & Gerhard 1985, Ebneter & Balick 1985, van Dokkum & Franx 1995, Tran et al. 2001, Lauer et al. 2004, Martel et al. 2004). Elliptical galaxies surrounded by shells have also been observed and are thought to be the result of a collision with a disk galaxy (Malin & Carter 1983, Quinn 1984, Michard & Prugniel 2004). Finally, a blue core, possibly experiencing star formation, has been detected in 30% of nearby Es (Abraham et al. 1999, Papovich et al. 2003, Menanteau et al. 2001, Goto 2005) and nuclear stellar disks in 60% of early-type galaxies (van den Bosch et al. 1994, Rest et al. 2001, Lauer et al. 2004).

Our knowledge of the detailed structure of elliptical galaxies is mostly based on what has been observed so far in the local Universe. The next step is to extend this study to higher redshift, so to describe in detail the galaxy structure - redshift correlation for ellipticals, and to complement this with an accurate study of their stellar populations. The high angular resolution of the Advanced Camera for Surveys (ACS) onboard HST allows for the very first time to measure the structural parameters of elliptical galaxies in the UDF/GRAPES surveys with redshifts between 0.5 and 1.3. In this paper, we discuss their star formation histories as derived from their GRAPES (GRISM ACS Program for Extragalactic Science, Pirzkal et al. 2004) spectra and their possible assembly histories as deduced from their isophotal structure in the UDF images. Hereafter, a concordance cosmology (Λ CDM, $\Omega_m = 0.3$, $H_0 = 70 \text{ km s}^{-1} \text{ Mpc}^{-1}$) is assumed.

2. observations

The Hubble Ultra Deep Field (UDF) is a survey of a $3^{0.4} \times 3^{0.4}$ field located in the Chandra Deep Field South, which was carried out with the Advanced Camera for Surveys (ACS) in four filters: F435W, F606W, F775W and F850LP (cf. Beckwith et al. 2005 for further details). We followed up these observations with ACS grism and slitless spectroscopy, as part of the GRAPES project which was awarded 40 HST orbits during Cycle 12 (ID 9793, P.I. S. Malhotra). The grism observations were taken at different epochs and at four different orientations in order to minimize the spectra contamination and overlapping from nearby sources. We have been then able to extract low resolution spectra ($R' \sim 100$, in the range 5500 Å to 10500 Å) for 5138 sources in the UDF field down to a limiting magnitude of $m_{F850LP} \sim 29.5$ in AB system. Readers are referred to Pirzkal et al. (2004) for a complete discussion of the data acquisition and reduction and for a description of the final GRAPES catalogue.

3. the sample of early-type galaxies

Our project aims at a combined analysis of the spectroscopic and morphological properties of early-type galaxies in the UDF. Hence, we selected from the GRAPES catalogue those sources with an early-type-like spectrum and bright enough to have an observed spectrum with a high signal-to-noise ratio, typically $\text{SNR} \geq 20$ per pixel at $\lambda = 8000 \text{ \AA}$. We found that this criterion imposes an apparent magnitude limit around $m_{F775W} = 24.0$ in AB system. The spectroscopic classification was performed visually, and 31 galaxies were selected. We then verified the accuracy of the classification by exploring concentration and asymmetry (CAS) to check whether these objects lie in the parameter space defined by ellipticals (cf. Conselice 2003). We computed the concentration (C) and asymmetry (A) parameters for the 31 spectroscopically classified galaxies in the F775W band, which roughly maps into a restframe B band at the redshifts reported in Table 1. We adopted for the concentration and asymmetry the same definitions and computing recipes given by Conselice (2003). For a consistency check, we show in Figure 1 the CAS parameters of our sample in the plane defined by Conselice et al. (2004), where the mean loci for nearby early-, late-type galaxies and mergers derived by Bershadsky et al. (2000) and Conselice et al. (2000) are also indicated. Our measurements are in good agreement with the distribution of galaxies at $0.2 < z < 1.3$ obtained by Conselice et al. (2004). We also visually inspected the images available for our sample in order to reject late-type galaxies whose bright bulge and/or bar would give CAS parameters very similar to those of ellipticals. We finally select as bona fide early-type galaxies those 18 objects (appearing as filled black circles in Figure 1), for which $C \geq 3.2$ and $A \leq 0.2$ in agreement with Conselice et al. (2004), and whose elliptical morphology was visually confirmed. As shown by Hamilton (1985), who selected ellipticals from their upper envelope colors, the 4000 Å break amplitude changes less than 7% in ellipticals up to $z \approx 0.8$, and the coevality among elliptical galaxies is within 2 Gyr between $z = 0$ and 1. In this respect then, our criteria give a rather consistent and robust selection of early-type galaxies.

Table 1 shows the main properties of our final sample, including the UDF/GOODS ID numbers. Magnitudes are given in the AB system (taking the MAG BEST values from SExtractor (Bertin & Arnouts 1996)). The optical magnitudes come from the UDF catalogue (Beckwith et al. 2005). Three of the galaxies in our sample (J033229.22-274707.6, J033240.33-274957.0, J033244.09-274541.5) are not in the UDF field of view although their spectra were detected in the GRAPES survey. Their images were extracted from the GOODS data (Giallisco et al. 2004). UDF 4527 and J033229.22-274707.6 have been also detected by Chandra in the soft X-rays, with a flux of $3 \times 10^{-17} \text{ erg s}^{-1} \text{ cm}^{-2}$ and $8 \times 10^{-17} \text{ erg s}^{-1} \text{ cm}^{-2}$ respectively (Alexander et al. 2003, Giacconi et al. 2002).

The last two columns of Table 1 give the spectroscopic redshifts derived with the ACS grism and with the VLT (FOR2: Vanzella et al. 2004, VIMOS: Le Fevre et al. 2004). The redshifts obtained from the ACS grism have been measured by matching templates corresponding to a range of stellar populations to the low resolution GRAPES spectra. For those galaxies with an

accurate VLT redshift, our grism estimates agreed to $z = (1+z)^{-1} < 0.01$, significantly better than any photometric redshift estimate (see e.g. Mozhayer et al. 2004). The bona fide early-type galaxies span the redshift range between $z \approx 0.5$ and 1.3. Notice here that 39% of the bona fide early-type galaxies are clustered around $z \approx 0.665$. This is a well known spike, since it has been detected in the K20 sample of ellipticals (Cimatti et al. 2002b), in the Chandra Deep Field South (Gilli et al. 2003) and in the VLT spectroscopic follow-up of GOODS (Vanzella et al. 2004). These surveys indicate that the galaxies at $z \approx 0.67$ constitute a loose structure rather than a cluster.

4. star formation histories

Our first approach in the study of the sample involves the star formation histories. In order to break the age-metallicity degeneracy, we combined models of galactic chemical enrichment and the low resolution slitless spectroscopy from the GRAPES data. We took extra care in avoiding contamination from nearby sources, which in some cases required the use of data corresponding to a single orientation.

In order to make a robust assessment of the ages and metallicities of the unresolved stellar populations, we decided to use two different models to describe the star formation histories, as described below. Briefly, the models depend on a reduced set of parameters, which uniquely determine a star formation history (SFH), i.e. a distribution of stellar ages and metallicities. This SFH is used to combine simple stellar populations from the models of Bruzual & Charlot (2003) and obtain a spectral energy distribution (SED) assuming a Salpeter IMF. Each choice of SFH is compared with the data via a χ^2 test. We explore a wide volume of parameter space in order to infer robust constraints on the ages and metallicities of the stellar populations in these galaxies. This comparison requires a careful process of degrading the synthetic SED (resolution $R \approx 2000$) to the (variable) resolution of the GRAPES spectra. Special care must be taken with respect to the change of the PSF with wavelength, which results in both an effective degradation of the spectral resolution as a function of wavelength, and a different net spectral resolution with respect to the size of the galaxy. The latter requires the spectral resolution to be treated as a free parameter, to be chosen by a maximum likelihood method. We found that this parameter is not degenerate with respect to those describing the star formation history, and mostly results in a global shift of the likelihood. The two models chosen to describe the build-up of the stellar component are as follows:

Model # 1 (EXP): We take a simple exponentially decaying star formation rate so that each history is uniquely parameterized by a formation epoch (which can be described by a formation redshift (z_F), a star formation timescale (τ) and a metallicity ($[M/H]$) which is kept fixed at all times.

Model # 2 (CSP): We follow a consistent chemical enrichment code as described in Ferreras & Silk (2000). The model allows for gas inflow and outflows and keeps the star formation efficiency as a free parameter. The metallicity evolves according to these parameters, using the stellar yields from Thielemann, Nomoto & Hashimoto (1996) for massive stars ($> 10 M_{\odot}$) and

van den Hoek & Groenewegen (1997) for intermediate mass stars. The free parameters are the star formation efficiency, the fraction of gas ejected in outflows, the formation epoch, and the timescale for the infall of gas.

Figure 2 shows the best fits and the observed SEDs. The error bars represent the observations and the solid line correspond to the best fits for the CSP model. Figure 3 shows the ages and metallicities of the best SFHs for each galaxy. Average and RMS scatter for age and metallicity are shown as dots and error bars, respectively. Notice the metallicity in the EXP models do not have an error bar as this model assumes a fixed value of metallicity for each SFH. The lines in the bottom panel give the age of the Universe as a function of redshift (solid line) and the ages at that redshift corresponding to a formation epoch of (dashed, from top to bottom) $z_F = f5;3;2g$. Analogously to the analysis of the surface brightness distribution shown in the next sections, we find that the stellar populations in these galaxies are dominated by old, passively evolving stars, formed at redshifts $z_F > 2$. Notice that the EXP model tends to underestimate the stellar ages. This model assumes a constant metallicity, which often forces older populations to have higher metallicities, which is compensated by the age-metallicity degeneracy by shifting the average towards younger ages. The more consistent model (CSP) generates a more realistic distribution of metallicities and we should expect it to be closer to the true populations. Nevertheless, the difference between these models is rather small, and we can safely reject a significant star formation at $z < 1.5$ in all galaxies. These models also give galaxy mass estimates in the range 9.5

$\log(M/M_\odot) = 11.5$, in agreement with the presence of massive stellar systems ($M > 10^{11} M_\odot$) at $z < 1$ as shown by Cimatti et al. (2002a).

The star formation histories that gives the best fit can be used to predict the evolution of the color-magnitude relation (CMR). Figure 4 shows the restframe $U - V$ vs. M_V CMR of our sample. The filled dots are simple translations of the observed photometry to restframe $U - V$ (i.e. a K correction) whereas the open dots evolve these galaxies to zero redshift, in order to compare our galaxies with local samples. Two characteristic error bars are shown. We plot Coma cluster galaxies from Bower, Lucey & Ellis (1992) and the dashed lines represent the linear fit and scatter. The Figure shows that our sample of early-type galaxies is fairly consistent with the stellar populations found in local elliptical galaxies. Notice that the passive fading of the brightest galaxies puts them at $z = 0$ within the luminosity range of the brightest local ellipticals. The available information also allows us to explore a projection of the Fundamental Plane, namely the Komendy relation (Komendy 1977). Figure 5 shows this relation (filled dots with error bars) compared to Coma cluster galaxies (squares; Jørgensen, Franx & Kjærgaard 1995), a sample of distant early-type galaxies in the HDF (grey dots; Fasano et al. 1998), the LBS radio elliptical galaxies at $z < 1.5$ (open stars; Waddington et al. 2002) and the early-type galaxies at $z < 2$ studied by Daddi et al. (2005, open dots). The translation from the observed photometry to B involves a K correction as well as the $(1+z)^4$ cosmological dimming. The offset $h_B = 1.5$ mag between our sample and Coma (as well as between Coma and the HDF sample

and the LBS radio galaxies) is compatible with the expected fading of the stellar populations. Notice that both the GRAPES and the HDF sample lack $r_{h1} > 10$ kpc galaxies, most likely due to the limited volume sample in the HDF and UDF surveys (the r_{h1} of the bona fide early-type galaxies was measured in the F775W filter, corresponding to the restframe B band at $z > 0.7$). No bona fide early-type galaxy at $z < 1$ is as compact as those studied by Daddi et al. (2005) at $z < 2$.

5. isophotal shapes

We used IRAF ELLIPSE routine (Jedrzejewski 1987) to measure the isophotal parameters of the bona fide early-type galaxies in the F606W, F775W and F850LP bands. At a mean redshift of 0.7 (cf. Table 1), these filters sample the restframe U, B and V bands. ELLIPSE allows the isophote center, ellipticity and position angle to vary at each iteration. Once a satisfactory fit is found, it computes the \sin and $\cos 3\theta$ and 4θ terms, which describe the deviations of the isophote from pure ellipse by means of the following Fourier expansion:

$$r(\theta) = r_0 \left[1 + \frac{a_3}{a} \cos(3\theta) + \frac{a_4}{a} \cos(4\theta) + \frac{b_3}{b} \sin(3\theta) + \frac{b_4}{b} \sin(4\theta) \right]$$

where θ is the position angle, r the distance from the galaxy center and a and b the semi-major and semi-minor axes. The a_4/a and a_3/a parameters, where a is the semi-major axis of the isophote, measure the deviations of the isophote from a pure ellipse. In particular, a_4/a measures the deviations symmetric with respect to the galaxy center (i.e. found along the isophote every 90°), while a_3/a the non-symmetric deviations occurring at every 120° .

We ran ELLIPSE leaving free the position of the center, the ellipticity (defined as $1 - b/a$, where a and b are the projected major and minor axes of a galaxy) and the position angle of the major axis and assuming a logarithmic step along the semi-major axis. The results are shown for each individual galaxy in Figures 17 to 34, where the surface brightness, ellipticity, position angle (PA) of the major axis, the a_3/a and a_4/a parameters are plotted for each filter as a function of distance from the galaxy center. These radial profiles extend to about 1.0^2 from the galaxy center in order to avoid overlap with nearby objects.

The ellipticity of the bona fide early-type galaxies show a variety of radial dependencies: increasing outward (i.e. J033229.22-274707.6, UDF 9264, UDF 2322, UDF 8, UDF 153, J033240.33-274957.0, J033244.09-274541.5), decreasing outward (UDF 3677), peaked (i.e. UDF 8316, UDF 6747, UDF 68, UDF 4587, UDF 4527, UDF 2107, UDF 5177), nearly flat (i.e. UDF 2387, UDF 1960, UDF 6027). In the case of UDF 1960, UDF 4587 and UDF 5177, the radial profile of the ellipticity is strongly perturbed by more compact (and usually bluer) sources projected onto the main body of these galaxies. These features are somewhat dependent on wavelength, since the ellipticity profiles appear to be smoother and to extend to lower values in the restframe V band (i.e. the F850LP filter). DiTullio (1978, 1979) analysed a sample of 75 nearby ellipticals and found that the radial variation of a galaxy ellipticity is different for different environments. Indeed, ellipticals with increasing ellipticity are found in galaxy clusters and groups, and systems with peaked ellipticity also in galaxy pairs. Ellipticals

with constant or decreasing ellipticity are preferentially isolated, although are also observed in galaxy clusters, groups and pairs. DiTullio (1978, 1979) suggested that an increasing ellipticity with radius could be a signature of merger and/or tidal interactions with a companion galaxy.

The position angle of the bona fide early-type galaxies is seen to generally vary with radius. The galaxies UDF1960, UDF3677, UDF68 and UDF8 show significant troughs in their PA profiles, which are likely due to the presence of dust lanes and compact sources projected onto the main body of these galaxies (cf. Sect. 7). Galletta (1980) explained the radial PA variations as the effect of the projection of a triaxial structure with the axes ratios (b/a and c/a) varying with radius, onto the plane of the sky. DiTullio (1979, 1980) proposed that PA variations larger than 10° could be relics of past mergers.

Isophotes can locally vary from a simple ellipse shape: if this variation occurs every 90° along the isophote and from the galaxy center, it indicates that the isophote has either a disk or a boxy shape. This variation is quantitatively measured with the a_4/a parameter; disk isophotes have $a_4/a > 0$, boxy isophotes are characterized by negative values of a_4/a , while elliptical isophotes have $a_4/a = 0$ (Lauer 1985, Bender et al. 1988, 1989). In our sample of bona fide early-type galaxies, the radial variation of the a_4/a parameter is quite dependent on wavelength, except for the galaxies UDF1960, UDF3677, UDF8316, UDF6747, UDF68, UDF2322, UDF6027 and UDF4527. The early-type galaxies which are clearly disk ($a_4/a \gg 0$) at any wavelength are: UDF2387, UDF6747, UDF4527, UDF2107 and UDF5177, while the only clear boxy galaxy is UDF3677. More elliptical galaxies (with no significant variations at any wavelength) are J033229.22-274707.6, UDF1960, UDF8316, UDF2322, UDF6027, J033240.33-274957.0. The galaxies mentioned above may show troughs or sharp peaks in the radial profile of their a_4/a parameter, which can be produced by dust lanes and compact sources projected onto the main body of these galaxies. UDF153 is the only galaxy that becomes boxy only in the restframe B and V bands (i.e. F775W and F850LP filters). Other galaxies feature a radial change from disk to boxy (and vice-versa), such as UDF9264, UDF68, UDF8, UDF4587 and J033244.09-274541.5. In particular, UDF8 changes from elliptical to disk in the restframe U and B bands (i.e. F606W and F775W filters), while it changes from boxy to disk in the restframe V band (F850LP filter). The radius at which this change occurs is in the area where the PSF still dominates the light distribution of the galaxy (cf. Sect. 5).

A second parameter, a_3/a , measures the deviation of an isophote from a perfect ellipse, every 120° along the isophote and from the galaxy center. This variation is mostly induced by the presence of dust lanes and clumps in the galaxy. Among the bona fide early-type galaxies, we detect $a_3/a \neq 0$ in UDF2387, UDF1960, UDF3677, UDF8316, UDF6747, UDF8, UDF6027, UDF153, UDF4587, UDF4527, J033244.09-274541.5, UDF2107 and UDF5177.

The measured isophotal parameters exhibit radial gradients that do not appear to significantly depend on the wavelength at which the galaxies were imaged. Given the

caveat on the effects of the morphological K-correction (Windhorst et al. 2002), this confirms the robustness of the criteria we used to select our sample of bona fide early-type galaxies.

Bender et al. (1988, 1989) analysed a sample of nearby ellipticals and concluded that they equally split among boxy systems (30%), disk galaxies (30%) and ellipticals with no significant deviations (30%). In particular, disk ellipticals have ellipticity larger than 0.25 and behave as oblate rotators, while boxy systems have ellipticities in the range between 0.15 and 0.45 and display a large variety of kinematical properties. In addition, boxy ellipticals are on average bigger with half-light radii larger than 5 kpc and brighter than disk systems in the B band, at radio wavelengths and in the X-rays. Starting from the idea whereby ellipticals can originate from the merger of two disk galaxies (Toomre & Toomre 1972), N-body simulations of disks collisions predict kinematic and photometric properties of the merger remnants very similar to those observed for elliptical galaxies, i.e. decoupled cores and isophotal shapes (cf. Barnes 1992, Hemquist 1992, Naab, Burkert & Hemquist 1999, Naab & Burkert 2003). Khochfar & Burkert (2004) have shown that the morphology of the merging galaxies and any subsequent episode of gas infall are critical in determining the shape of the merger remnant. Boxy ellipticals can be reproduced via a merger of two equally-massive disk galaxies or a major merger of two early-type galaxies. Disk ellipticals are mainly formed through an unequal-mass merger of two disk galaxies or late gas infall. In the hierarchical framework equal-mass mergers are expected to be much rarer than the unequal-mass, although the observational selection seems to go in the opposite direction (i.e. the ratio of boxy to disk galaxies at $z' = 0$ is nearly one).

6. average isophotal parameters

Given that the bona fide early-type galaxies in the UDF/GRAPES survey are at higher redshift than the nearby ellipticals studied by Bender et al. (1988, 1989), it is interesting to check whether the isophotal parameters show any change with redshift. We therefore computed for each galaxy the characteristic ellipticity and isophotal twist PA, the mean a_3/a and a_4/a parameters ($ha_3=ai$ and $ha_4=ai$) following the prescriptions of Bender et al. (1988) and in the F850LP filter which for the observed redshifts corresponds to the restframe V and R bands used by Bender et al. Briefly, we averaged the a_3/a and a_4/a values measured at $R_i \leq r \leq R_o$ weighted by their errors and by the counts in the isophote at each isophotal mean radius r . Here, R_o is 1.5 times the half-light radius r_{11} derived from the F850LP radial profile and R_i is the radius corresponding to 3 times the FWHM of the PSF in the F850LP filter, chosen to avoid the central part of a galaxy where the light distribution is perturbed by the PSF. While R_i is 12 pixels, i.e. $0''.36$, R_o ranges from $0''.55$ to $1''.25$. The isophotal twist was measured as a difference in PA between R_i and R_o , while the characteristic ellipticity was taken equal to the ellipticity at the half-light radius in case of increasing, decreasing or flat radial profiles, or equal to the peak ellipticity in case of peaked radial profiles. The final results are reported in Table 2, where the $ha_3=ai$ and $ha_4=ai$ values have been multiplied by 100. Since its R_o is comparable to R_i , we

could not determine the isophotal parameters of UDF 68. As pointed out by Odehahn et al. (1997), the S/N ratio in the images can affect the measurement of the galaxy projected a and b axes and hence its ellipticity, in the sense that galaxies with a lower S/N value are measured to be rounder than real. Therefore, to test the reliability of the isophotal parameters derived for our sample, we measured the ellipticity, $ha_3=ai$ and $ha_4=ai$ parameters for a number of simulated ellipticals. The simulations were performed (cf. Appendix A) using a Sersic profile with index between 3 and 4, and assuming the S/N ratio and the integrated magnitude of the observed data. The simulated images were then convolved with the ACS PSF in the F775W filter. We were able to recover for the simulated images not convolved by the PSF isophotal parameters very close to their input values, thus indicating that the S/N ratio of the data does not significantly affect our measurements. We also found that the ACS PSF underestimates the ellipticity by $\sim 10\%$ and introduces a scatter in $ha_3=ai$ and $ha_4=ai$ of about 0.2 and 0.15 respectively around the input values used for the simulations ($a_3/a = a_4/a = 0$).

The isophotal parameters of the bona fide early-type galaxies (black filled circles), corrected for the above errors, are plotted in Figure 6 as a function of the galaxy half-light radius $r_{h,1}$ (measured in the F850LP filter, corresponding to the restframe V band at $\langle z \rangle \sim 0.7$), total absolute magnitude in restframe B band M_B , and compared with the sample of Bender et al. (1988, 1989) represented with grey filled circles. It has to be specified that the M_B values were derived from the best-fitting model spectra (cf. Sect. 4), also K-corrected. The magnitude range (hence stellar mass) of the nearby ellipticals is nicely sampled by the bona fide early-type galaxies, and this makes the comparison of the two galaxy samples in their isophotal parameters even more robust. Overall, the bona fide early-type galaxies confirm the trends traced by nearby ellipticals:

- i) boxy ellipticals tend to be bigger (as shown in Figure 6a).
- ii) Rounder ellipticals show smaller deviations from pure ellipses, while larger deviations are seen in galaxies with ellipticity > 0.25 . Disky ellipticals have $0.15 < ha_4=ai < 0.6$, while boxy ellipticals $0.15 < ha_4=ai < 0.45$. The deviant galaxies in our sample are UDF 1960 and J033240.33-274957.09 (cf. Figure 6b). The ellipse fitting of UDF 1960 is affected by the presence of a blue clump (a probable lens candidate, cf. Sect. 7.4) at a distance of $0.4''$ from the galaxy center, and by low S/N values in the case of J033240.33-274957.0.
- iii) Boxy ellipticals tend to be brighter than disk systems (see Figure 6c).

Although not shown in Figure 6, the isophotal twist increases at lower ellipticity because of the uncertainties in determining the major axis PA of a rounder galaxy. We can thus conclude that ellipticity and $ha_4=ai$ do not significantly change with redshift up to $z \sim 1$. One third of the bona fide early-type galaxies are characterized by values of $ha_3=ai$ larger than the range spanned by nearby ellipticals. These are: UDF 1960, UDF 2107, UDF 2387, UDF 3677, UDF 4587 and J033240.33-274957.0. Their large $ha_3=ai$ values are likely due to the presence of dust lanes (UDF 2387 and UDF 3677, cf. Sect. 7.1) or blue clumps close to the galaxy center (UDF 4587 and

UDF 2107, cf. Sect. 7.3; UDF 1960 with an overlapping lens candidate is a special case, cf. Sect. 7.4).

7. substructures in the udf early-type galaxies

We used the outputs of the ELLIPSE routine to build model images of the bona fide early-type galaxies, and subtracted them from the observed frames in order to look for residual substructures. In the cases where substructures were detected, we re-ran ELLIPSE masking out the substructures and adjusted the mask every run until the extinction map of each galaxy reached a minimum value of ~ 0.05 mag in the unmasked pixels. The extinction map was computed from the ratio of the observed image to the ELLIPSE model image with the formula: $2.5 \cdot \log(\text{Observed}/\text{Model})$. We applied this procedure to the images obtained in the F606W and F775W filters, which are characterized by a better S/N ratio and PSF with respect to the F435W and F850LP filters.

In this way, we could detect dust lanes, disks and clumps in a significant fraction of our sample. Six galaxies do not show either a disk structure nor dust lanes: J033229.22-274707.6, J033240.33-274957.0, J033244.09-274541.5, UDF 2322, UDF 6027 and UDF 8316. J033244.09-274541.5 is shown in Figure 7: its (V-I) color map is in the left-hand side panel, a close-up of the central region ($1.2'' \times 1.2''$) in the F775W filter is in the middle panel in units of counts/s, and the extinction map of the same region in units of magnitude (mean residual value ~ 0.05 mag/pix) in the right-hand side panel. The (V-I) color maps of the other five featureless galaxies are shown in Figures 8 and 9. The (V-I) color maps were obtained using Voronoi tessellations, so that pixels were binned in order to reach a chosen and constant S/N ratio per bin (cf. Cappellari & Copin, 2003). In our case, the targeted S/N ratio is 0.05 mag the color uncertainty.

7.1. Dust lanes

Dust lanes have been resolved in UDF 2387 and UDF 3677 (see Figures 10 and 11). They appear as white stripes in the extinction maps (right-hand side panels of both Figures). Here, grey indicates a residual of about 0.05 mag and white an extinction A_{F775W} (restframe A_B) up to ~ 0.25 mag in UDF 2385 and 0.18 mag in UDF 3677. These values are very similar to what found for dusty nearby ellipticals at $z \sim 0$ by Sadler & Gerhard (1985).

7.2. Disks

UDF 4527 and UDF 6747 are characterized by a disk-like structure that is aligned with the galaxy major axis and has a full extension of about $1''$ (corresponding nearly to the half-light radius of each galaxy). These features are shown in the right-hand side panels of Figures 12 and 13, where they turn out to be in emission (black pixels) by ~ 0.10 mag/pix in UDF 4527 and 0.25 mag/pix in UDF 6747. In these images, light grey levels indicate residuals of about ~ 0.05 mag. In the (V-I) [restframe (B-V)] color map of UDF 4527 and UDF 6747, the disk turns out to be as red as the galaxy and the two should thus be coeval. Such a similarity is known to be common among S0 galaxies, because of either small age differences (Peltier & Balcells 1996) or a larger amount of dust in the disk (Michard & Poulain 2000).

7.3. Blue clumps

As seen in Figures 7 to 16, a large fraction of bona fide early-type galaxies shows compact, blue clumps at different distances (up to $2''$) from the galaxy center. UDF6747, in particular, is surrounded by a cluster of blue clumps at one edge of its major axis (cf. Figure 12). Figure 15 highlights this feature in UDF153. We could measure the integrated magnitude of these clumps in the filters of the UDF after having subtracted the ELLIPSE model image from the observed frame of each galaxy. It turns out that these clumps are very faint, with magnitudes between 30.9 and 26.1, and contribute to the total flux of the host galaxy at a 4% level. Hence, these clumps do not contribute significantly to the grism spectra of the bona fide early-type galaxies. What is the nature of the blue clumps? The simplest explanation would be that they are sources at high redshift, as in the case of UDF1960, where the blue clump (cf. Figure 14) is a lens candidate (Fassnacht et al. 2004). On the other hand, given the number of objects detected in the UDF field and the size of the galaxies in our sample, we have estimated a probability of about 30% for objects to overlap. A more intriguing possibility is that the most compact of these clumps are physically associated with the bona fide early-type galaxies, and, as such, may be H II regions or young star clusters or satellite dwarf galaxies. To test this hypothesis, we ran the Hyperz code (Bolzonella et al. 2000) on the set of magnitudes measured for each clump, assuming that the clump is at the same redshift of the galaxy in which it has been observed. The reduced χ^2 of the fits indicates that some of these clumps could be consistent with the above constraint, and they could be young (few 10^6 – few 10^8 yrs) systems in the range $-12 < M_V < -16$. Though speculative, these results are in good agreement with the study of O'Dea et al. (2001) who found four star-forming regions in the double-double radio galaxy 3C 236, and of Yang et al. (2004) who detected blue compact sources in ve E+A galaxies at $z' < 0.1$.

7.4. Peculiar features

UDF68, UDF1960, UDF2107 and UDF5177 display in their extinction map some arc-like features in emission. An example is given in Figure 16 for UDF5177. With the data in hand, it is not possible to establish whether these features are real substructures or, for example, lensed sources at high redshifts overlapping with the UDF early-type galaxies. Fassnacht et al. (2004) have identified only one lens candidate among the bona fide early-type galaxies, which lies nearby UDF1960. We suggest that UDF68 has also lensed sources projected onto its main body, given that the morphology of its (V-I) map is quite similar to UDF1960.

7.5. Blue cores

Two galaxies in our sample exhibit a blue core: UDF5177 (cf. Figure 16) and UDF6027 (cf. Figure 8). About 30% of nearby ellipticals have a blue core, which is usually believed to have experienced recent star formation (Abraham et al. 1999, Papovich et al. 2003, Menanteau et al. 2001, Goto 2005). Menanteau et al. (2004) have found a "blue-core" elliptical at $z = 0.624$ which seems to host an AGN. In our sample, UDF5177 and UDF6027 are at $z = 0.50$ and 1.32 , respectively.

8. conclusions

According to the current paradigm of galaxy formation, elliptical galaxies form through the merger of disk galaxies. As shown by Kaumann & Charlot (1998) this predicts a fairly extended formation history, which is difficult to reconcile with the old stellar age and the enhanced chemistry of these galaxies. Because of a prolonged merger history, one would expect the isophotal morphology of early-type galaxies to be more distorted at high redshift compared to nearby ellipticals. In this respect, the UDF survey is an unique dataset which allows, for the very first time, to measure accurate isophotal parameters for 18 bona fide early-type galaxies between $z' = 0.5$ and 1.3 . At the same time, the GRAPES survey provides for these same objects high S/N grism spectra, which are used to determine their stellar age and formation redshifts. The population of $z > 1$ early-type galaxies in the UDF is clearly old. The analysis of their spectra indicates that their stellar populations are rather homogeneous in age and metallicity and formed at redshifts $z_F = 2 - 5$. Evolving them passively, they become indistinguishable from the ellipticals observed in the Coma cluster [cf. also Daddi et al. (2005) for a sample of UDF early-type galaxies at $z = 2$]. As discussed by Hamilton (1985), spectroscopically-selected early-type galaxies are generally seen long after (i.e. $>> 1$ Gyr) the last major merger. After such a merger, these objects quickly settle back to their quasi-steady-state, and will then look for a much longer time like non-evolving ellipticals: it is during this phase that we select and observe them now.

The $z > 1$ early-type galaxies in the UDF are morphologically very similar to nearby ellipticals. They separate into disky galaxies (53% with $ha_4=ai > 0.2$), boxy galaxies (23% with $ha_4=ai < -0.2$) and systems with no significant deviation from a pure ellipse (23% with $-0.2 < ha_4=ai < 0.2$). Given the small field of view of the UDF and therefore the small sample, these fractions can be taken as in good agreement with the results of Bender et al. (1988, 1989) who found 30% of the nearby ellipticals to be disky, 30% boxy and 30% with no significant deviations. The slight overabundance of disky vs boxy ellipticals in our sample could be explained by their environment. Indeed, VLT spectroscopic follow-up has detected three large-scale structures in the UDF (at $z' = 0.67, 0.73, 1.10$ and 1.61 , Vanzella et al. 2004, see also Cimatti et al. 2002 and Gilli et al. 2003) which make the UDF an over-dense region at any of these three redshifts. In over-dense regions, the N-body simulations of Kochhar & Burkert (2004) predict a higher number of disky vs boxy ellipticals. The isophotal structure of the bona fide early-type galaxies obeys the correlations already observed among nearby ellipticals: i) disky ellipticals have generally higher characteristic ellipticities; ii) boxy ellipticals have larger half-light radii and are brighter in the B band. In this respect, the isophotal shape of ellipticals does not significantly change between $z = 0$ and 1 . This suggests that these galaxies either do not accrete significantly in their evolution towards $z = 0$, or mergers at later redshifts do not vary the percentages of disky and boxy ellipticals. Both cases could agree with the results of Treu et al. (2005), who have shown that massive ellipticals ($10^{11.5} M_\odot$) accreted less than 1% of their mass

since $z' > 1$, while ellipticals with masses smaller than $10^{11} M_{\odot}$ accreted about 20–40%. In this respect, also Schade et al. (1999) suggested that less than 5% of the stellar mass in ellipticals has been formed since $z = 1$ and that merging is not required since $z = 1$ to produce the present-day space density of ellipticals.

The $h_{\alpha} = a_i$ parameter appears to be larger than measured by Bender et al. for nearly one third of the bona fide early-type galaxies. This deviation is likely due to the presence of dust lanes (in 10% of the sample, a percentage a factor of 4 smaller than observed at $z = 0$) and most notably of clumps close to the galaxy center. Blue (in the $(V-I)$ color) clumps have been detected in about 50% of the bona fide early-type galaxies, at different distances from the center (up to $2''$, in the galaxy outskirts). From their photometry and under the assumption that they are at the same redshift as their host galaxies, we have derived ages (from few 10^6 to few 10^8 yrs) and luminosities ($-12 < M_V < -16$) consistent with them being either young star clusters or dwarf irregular galaxies. They appear very similar to the blue compact sources observed in $E+A$ galaxies at $z' > 0.1$ by Yang et al. (2004), who suggested these sources to be young star clusters. On the other hand, the hypothesis of being dwarf galaxies would put these blue clumps in the right mass range to explain the low-mass accretion history of ellipticals more massive than $10^{11.5} M_{\odot}$ (i.e. these galaxies seem to have accreted less than 1% of their mass since $z' > 1$ according to the results of Treu et al. 2005, or less than 5% as discussed by Schade et al. 1999). Gas accretion is also invoked to explain the presence of four star-forming regions in the double-double radio galaxy 3C 236; their age difference would compare with the timescale of the nuclear activity in this galaxy and hence would set time constraints on the infall of gas experienced by 3C 236 (O'Dea et al. 2001).

To add more speculation to the picture, since the blue clumps in our sample galaxies are distributed at different distances from the galaxy center, we could imagine that they have been accreted and may possibly sink to the galaxy center, forming a blue core as observed in UDF 5177 at $z' > 0.5$. Clearly, a dedicated spectroscopic campaign would be needed to unveil the true nature of these blue clumps.

In the sample of bona fide early-type galaxies, UDF 153 is particularly remarkable, since it is surrounded by a faint and incomplete shell. As shown by Quinn (1984), such a shell is the relic of a relatively recent merger with a smaller disk galaxy and can be observed for about 1 Gyr. The high phase-space density of a disk galaxy is indeed required to produce such a spatially confined substructure as the observed shells are. The GRAPES spectrum of UDF 153 indicates a redshift of 0.98, suggesting that the merger possibly occurred at $z = 1$. This would also imply that some disk galaxies were already in place at $z = 1$, despite observations which show that the fraction of disk galaxies rapidly decreases at $z > 1$ (Bell et al. 2005).

N-body simulations (cf. Khorfar & Burkert 2004, Jesseit et al. 2005) indicate that the boxiness/diskiness shape of an elliptical galaxy is a long-lived signature of a merger if no further disturbances (i.e. late gas infall and/or subsequent mergers) occur. Indeed, the stellar orbits which forge the a_4/a parameter are stable and in equilibrium. Therefore, if the system stays unperturbed after the major merger which formed it, the "lifetime" of its isophotal shape is comparable with the age of its stellar population. Moreover, the isophotal shape of the merger remnant depends on the mass ratio of the merger and on the morphology (i.e. stellar orbits) of the merging galaxies. Given that the fractions of disky and boxy systems among the bona fide early-type galaxies is similar to what observed at $z = 0$, and modulo the small size of their sample, the bona fide early-type galaxies can be used to trace the mass ratio of mergers as a function of redshift and the lifetime of the different isophotal shapes taken by ellipticals in N-body simulations like those of Khorfar & Burkert.

A last comment is devoted to the masses of the bona fide early-type galaxies. Our spectroscopic analysis indicates masses between $10^{9.5}$ and $10^{11.5} M_{\odot}$ in stars, which likely formed at about $z' > 3$. At this redshift, such masses are consistent with Lyman-break galaxies (LBG, Steidel et al. 1996, Shapley et al. 2001, Papovich et al. 2001), SCUBA galaxies (Bertoldi et al. 2000, Smail et al. 2002, Genzel et al. 2003, Webb et al. 2003, Chapman et al. 2003, 2004) and bright radio galaxies (van Breugel et al. 1998, Dey et al. 1997). These galaxies are all observed undergoing intense star formation with a rate varying from $90 M_{\odot} \text{ yr}^{-1}$ (in LBGs, Shapley et al. 2001) up to $500 M_{\odot} \text{ yr}^{-1}$ (in SCUBA sources, Genzel et al. 2003) and $1000 M_{\odot} \text{ yr}^{-1}$ (in high-redshift radio galaxies, Dey et al. 1997). Such a star-formation rate is able to enrich the galactic ISM up to a metallicity of about $0.4 Z_{\odot}$ (Pettini et al. 2001), a value very similar to what found in this paper for the bona fide early-type galaxies. Such starbursts are also likely to produce the α -element enhancement typical of elliptical galaxies (Trager et al. 2000). These similarities in mass and metallicity add further evidence to the evolution of vigorously star-forming galaxies at high redshift into $z' > 1$ ellipticals.

We would like to thank A. Burkert, F.C. van den Bosch and C. Porciani for valuable discussions. ED acknowledges support from NASA through the Spitzer Fellowship Program, under award 1268429. The imaging and spectroscopy data are based on observations with the NASA/ESA Hubble Space Telescope, obtained at the Space Telescope Science Institute, which is operated by AURA Inc., under NASA contract NAS 5-26555. This work was supported by grant G0-09793.01-A, G0-09793.03-A and G0-09793.08-A from the Space Telescope Science Institute. This project has made use of the aXe extraction software, produced by ST-ECF, Garching, Germany.

REFERENCES

- Abraham, R.G., Ellis, R.S., Fabian, A.C. et al., 1999, MNRAS, 303, 641
 Abraham, R.G., van den Bergh, S., Gazebrook, K. et al., 1996, ApJS, 107, 1
 Alexander, D.M., Bauer, F.E., Brandt, W.N. et al., 2003, AJ, 126, 539
 Bames, J.E., 1992, ApJ, 393, 484
 Beckwith, S.V.W. et al., 2005, in preparation

- Bell, E.F., Papovich, C., Wolf, C. et al., 2005, *ApJ* submitted, astro-ph/0502246
- Bender, R., D'Onofrio, S., Mollenho, C., 1988, *A & A Suppl. Ser.*, 74, 385
- Bender, R., Summa, P., D'Onofrio, S., Mollenho, C., Madae, J., R., 1989, *A & A*, 217, 35
- Bemardi, M., Sheth, R.K., James, A. et al., 2003, *AJ*, 125, 1882
- Bershady, M.A., Jangren, J.A., Conselice, C.J., 2000, *AJ*, 119, 2645
- Bertin, E. & Amouts, S., 1996, *A & S*, 117, 393
- Bertoldi, F., Carilli, C.L., Menten, K.M. et al., 2000, *A & A*, 360, 92
- Bolzonella, M., Miralles, J.-M., Pello, R., 2000, *A & A*, 363, 476
- Brichmann, J., Ellis, R.S., 2000, *ApJ*, 536, L77
- Bruzual, G. & Charlot, S., 2003, *MNRAS*, 344, 1000
- Caon, N., Capaccioli, M., D'Onofrio, M., 1993, *MNRAS*, 265, 1013
- Cappellari, M., Copin, Y., 2003, *MNRAS*, 342, 345
- Camatti, A., Daddi, E., Mignoli, M. et al., 2002a, *A & A*, 381, 68
- Camatti, A., Mignoli, M., Daddi, E. et al., 2002b, *A & A*, 392, 395
- Chapman, S.C., Blain, A.W., Ivison, R.J., Smail, I., 2003, *Nature*, 422, 695
- Chapman, S.C., Windhorst, R.A., Odewahn, S., Yan, H., Conselice, C.J., 2004, *ApJ*, 599, 92
- Colley, W.N., Rhoads, J.E., Ostriker, J.P., Spergel, D.N., 1996, *ApJ*, 473, L63
- Conselice, C.J., 2003, *ApJS*, 147, 1
- Conselice, C.J., Bershady, M.A., Jangren, J.A., 2000, *ApJ*, 529, 886
- Conselice, C.J., Blackburne, J.A., Papovich, C., 2004, astro-ph/0405001
- Daddi, E., Renzini, A., Pirzkal, N. et al., 2005, *ApJ* accepted
- Davies, R.L., Kuntschner, H., Emmesley, E. et al., 2001, *ApJ*, 548, L33
- Dey, A., van Breugel, W.J.M., Vacca, W., Antonucci, R., 1997, *ApJ*, 490, 698
- de Zeeuw, T., Bureau, M., Emmesley, E. et al., 2002, *MNRAS*, 329, 513
- DiTullio, G.A., 1978, *A & A*, 62, L17
- DiTullio, G.A., 1979, *A & A Suppl. Ser.*, 37, 591
- van Dokkum, P.G., Franx, M., 1995, *AJ*, 110, 2027
- Dressler, A., 1980, 236, 351
- Dressler, A., Oemler, A.G.Jr., Couch, W.J. et al., 1997, *ApJ*, 490, 577
- Driver, S.P., Fernandez-Soto, A., Couch, W.J. et al., 1998, *ApJ*, 496, 93
- Driver, S.P., Windhorst, R.A., Griest, R., 1995, *ApJ*, 453, 48
- Ebner, K., Balick, B., 1985, *AJ*, 90, 183
- Eggen, O.J., Lynden-Bell, D., Sandage, A.R., 1962, *ApJ*, 136, 748
- Fasano, G., Cristiani, S., Amouts, S., Filippi, M., 1998, *AJ*, 115, 1400
- Fassnacht, C.D., Moustakas, L.A., Casertano, S. et al., 2004, *ApJ*, 600, L155
- Ferreras, I. & Silk, J., 2000, *MNRAS*, 316, 786
- Franx, M., 1988, *MNRAS*, 231, 285
- Galletta, G., 1980, *A & A*, 81, 179
- Genzel, R., Baker, A.J., Tacconi, L.J. et al., 2003, *ApJ*, 584, 633
- Giacconi, R., Zimm, A., Wang, J.X. et al., 2002, *ApJS*, 139, 369
- Giallisco, M., Ferguson, H.C., Koekemoer, A.M. et al., 2004, *ApJ*, 600, 93
- Gilli, R., Camatti, A., Daddi, E. et al., 2003, *ApJ*, 592, 721
- Glazebrook, K., Ellis, R., Santiago, B., Griest, R., 1995, *MNRAS*, 275, L19
- Goto, T., 2005, *MNRAS* submitted, astro-ph/0503088
- Graham, A., Erwin, P., Caon, N., Trujillo, I., 2001, *ApJ*, 563, L11
- Graham, A., Lauer, T.R., Colless, M., Postman, M., 1996, *ApJ*, 465, 534
- Hamilton, D., 1985, *ApJ*, 297, 371
- Hemquist, L., 1992, *ApJ*, 400, 460
- Jedrzejewski, R.J., 1987, *MNRAS*, 226, 747
- Jesseit, R., Naab, Y., Burkert, A., 2005, submitted to *MNRAS*, astro-ph/0501418
- Jorgensen, I., Franx, M. & Kjergaard, P., 1995, *MNRAS*, 273, 1097
- Kaumann, G. & Charlot, S., 1998, *MNRAS*, 297, L23
- Khochfar, S., Burkert, A., 2004, submitted to *MNRAS*, astro-ph/0409705
- Komendy, J., 1977, *ApJ*, 218, 333
- Lauer, T.R., 1985, *MNRAS*, 216, 429
- Lauer, T.R., Faber, S.M., Gebhardt, K. et al., 2004, *AJ*, submitted, astro-ph/0412040
- LeFevre, O., Guzzo, L., Meneux, B. et al. *A & A*, astro-ph/0403628
- Longo, G., Busarello, G., Capaccioli, M., Bender, R., 1989, *A & A*, 225, 17
- Malin, D.F., Carter, D., 1983, *ApJ*, 274, 534
- Marlet, A.R., Ford, H.C., Bradley, L.D. et al., 2004, *AJ*, accepted, astro-ph/0411148
- Menanteau, F., Abraham, R.G. & Ellis, R.S., 2001, *MNRAS*, 322, 1
- Menanteau, F., Marlet, A.R., Tozzi, P. et al., 2004, *ApJ*, accepted, astro-ph/0411125
- Michard, R., Poulain, P., 2000, *A & S*, 141, 1
- Michard, R., Pagniel, P., 2004, *A & A*, 423, 833
- Mobasher, B., Idzi, R., Benitez, N. et al., 2004, *ApJ*, 600, L167
- Naab, T., Burkert, A., 2003, *ApJ*, 597, 893
- Naab, T., Burkert, A. & Hemquist, L., 1999, *ApJ*, 523, L133
- Odewahn, S.C., Koekemoer, A.M., Baum, S.A. et al., 2001, *ApJ*, 121, 1915
- Odewahn, S.C., Burstein, D., Windhorst, R.A., 1997, *AJ*, 114, 2219
- Papovich, C., Dickinson, M., Ferguson, H.C., 2001, *ApJ*, 559, 620
- Papovich, C., Giallisco, M., Dickinson, M. et al., 2003, *ApJ*, 598, 827
- Peletier, R.F., Balcells, M., 1996, *AJ*, 111, 2238
- Pettini, M., Shapley, A.E., Steidel, C.C. et al., 2001, *ApJ*, 554, 981
- Pirzkal, N., Xu, C., Malhotra, S. et al., 2004, *ApJS*, 154, 501
- Quinn, P.J., 1984, *ApJ*, 279, 596
- Rest, A., van den Bosch, F.C., Jaew, W. et al., 2001, *AJ*, 121, 2431
- Sadler, E.M., Gerhard, O.E., 1985, *MNRAS*, 214, 177
- Sersic, J.-L., 1968, *Atlas de Galaxias Australes* (Cordoba: Obs. Astron.)
- Schade, D., Lilly, S.J., Crampton, D. et al., 1999, *ApJ*, 525, 31
- Shapley, A.E., Steidel, C.C., Adelberger, K.L., Dickinson, M., Giallisco, M., Pettini, M., 2001, *ApJ*, 562, 95
- Smail, I., Ivison, R.J., Blain, A.W., Kneib, J.-P., 2002, *MNRAS*, 331, 495
- Stanford, S.A., Eisenhardt, P.R. & Dickinson, M., 1998, *ApJ*, 492, 461
- Steidel, C.C., Giallisco, M., Pettini, M., Dickinson, M., Adelberger, K.L., 1996, *ApJ*, 462, L17
- Thielmann, F.-K., Nomoto, K. & Hashimoto, M., 1996, *ApJ*, 460, 408
- Thomas, D., Gallego, L. & Bender, R., 1999, *MNRAS*, 302, 537
- Thomas, D., 1999, *MNRAS*, 306, 655
- Toomre, A., Toomre, J., 1972, *ApJ*, 178, 623
- Trager, S.C., Faber, S.M., Worthey, G., Gonzalez, J.J., 2000, *AJ*, 119, 1645
- Tran, H.D., Svetanov, Z., Ford, H.C. et al., 2001, *AJ*, 121, 2928
- Treu, T., Ellis, R.S., Liao, T.X. et al., 2005, *ApJ* submitted, astro-ph/0503164
- van Breugel, W.J.M., Stanford, S.A., Spinrad, H., Stem, D., Graham, J.R., 1998, *ApJ*, 502, 614
- van den Bosch, F.C., Ferrarese, L., Jaew, W., Ford, H.C., O'Connell, R.W., 1994, *AJ*, 108, 1579
- van den Hoek, L.B. & Groenewegen, M.A.T., 1997, *A & S*, 123, 305
- Vanzella, E., Cristiani, S., Dickinson, M. et al. 2004, *A & A*, in press, astro-ph/0406591
- Yang, Y., Zabudo, A.I., Zaritsky, D., Lauer, T.R., Mihos, J.C., 2004, *ApJ*, accepted, astro-ph/0402062
- Waddington, I., Windhorst, R.A., Cohen, S.H. et al., 2002, *MNRAS*, 336, 1342
- Webb, T.M., Eales, S.A., Lilly, S.J. et al., 2003, *ApJ*, 587, 41
- Williamson, R.E., Balick, B., Dickinson, M. et al., 1996, *AJ*, 112, 1335
- Windhorst, R.A., Taylor, V.A., Jansen, R.A. et al., 2002, *ApJS*, 143, 113
- Worthey, G., 1994, *ApJS*, 95, 107

Table 1. The sample: UDF/GOODS IDs, coordinates and magnitudes (A B)

ID	RA (J2000)	Dec (J2000)	F 435W	F 606W	F 775W	F 850LP	z_{GRISM}	z_{VLT}	
J033229.22	274707.6	03:32:29.2	27:47:07.6	22.22	22.86	20.97	20.99	0.67	0.67
UDF 2387		03:32:35.8	27:47:58.8	24.52	22.13	20.74	20.29	0.66	0.66
UDF 1960		03:32:36.0	27:48:11.9	23.95	22.55	21.59	21.29	0.60	0.60
UDF 9264		03:32:37.2	27:46:08.1	22.78	23.46	21.96	20.89	1.07	1.10
UDF 3677		03:32:37.3	27:47:29.3	24.21	21.74	20.30	19.81	0.65	0.67
UDF 8316		03:32:38.4	27:46:31.9	22.33	23.48	22.21	21.78	0.62	
UDF 6747		03:32:38.8	27:46:48.9	25.22	23.03	21.73	21.28	0.54	0.62
UDF 68		03:32:38.8	27:49:28.5	26.83	24.49	22.98	22.36	0.82	
UDF 2322		03:32:39.2	27:47:58.4	24.93	22.49	21.07	20.62	0.66	
UDF 8		03:32:39.5	27:49:28.3	24.85	22.68	21.39	20.96	0.65	
UDF 6027		03:32:39.6	27:47:09.1	26.19	24.96	23.71	22.79	1.15	1.32
UDF 153		03:32:39.6	27:49:09.6	25.15	22.95	21.51	20.63	0.98	0.98
J033240.33	274957.0	03:32:40.3	27:49:57.0	23.51	22.23	21.88	21.88	0.66	
UDF 4587		03:32:40.7	27:47:31.0	23.99	22.96	21.67	21.22	0.67	0.67
UDF 4527		03:32:41.4	27:47:17.2	24.42	22.41	21.06	20.61	0.62	
J033244.09	274541.5	03:32:44.1	27:45:41.5	23.11	21.12	20.09	19.75	0.49	
UDF 2107		03:32:45.8	27:48:12.9	24.42	22.77	21.76	21.38	0.62	0.53
UDF 5177		03:32:48.5	27:47:19.6	24.74	23.33	22.43	22.08	0.50	

Table 2. The isophotal parameters of the bona fide early-type galaxies. These have not been corrected for the errors derived in the Appendix.

ID	Ellipticity	$ha_3=ai$ 100	$ha_4=ai$ 100	PA
J033229.22-274707.6	0.12	0.06	0.11	7.35
UDF 2387	0.14	-0.79	0.64	15.29
UDF 1960	0.18	7.70	5.09	0.00
UDF 9264	0.20	-0.13	-0.22	0.44
UDF 3677	0.08	-0.63	-0.42	6.40
UDF 8316	0.20	-0.05	-0.25	0.44
UDF 6747	0.30	0.32	2.44	4.24
UDF 68				
UDF 2322	0.13	0.29	0.09	2.32
UDF 8	0.21	-0.27	0.05	0.98
UDF 6027	0.06	0.07	-0.04	68.29
UDF 153	0.22	-0.06	-1.03	15.90
J033240.33-274957.0	0.16	-0.69	3.05	7.29
UDF 4587	0.45	-0.53	0.46	1.12
UDF 4527	0.38	-0.04	1.80	6.90
J033244.09-274541.5	0.30	-0.17	0.51	7.00
UDF 2107	0.21	-0.76	1.62	1.46
UDF 5177	0.16	-0.12	0.44	48.61

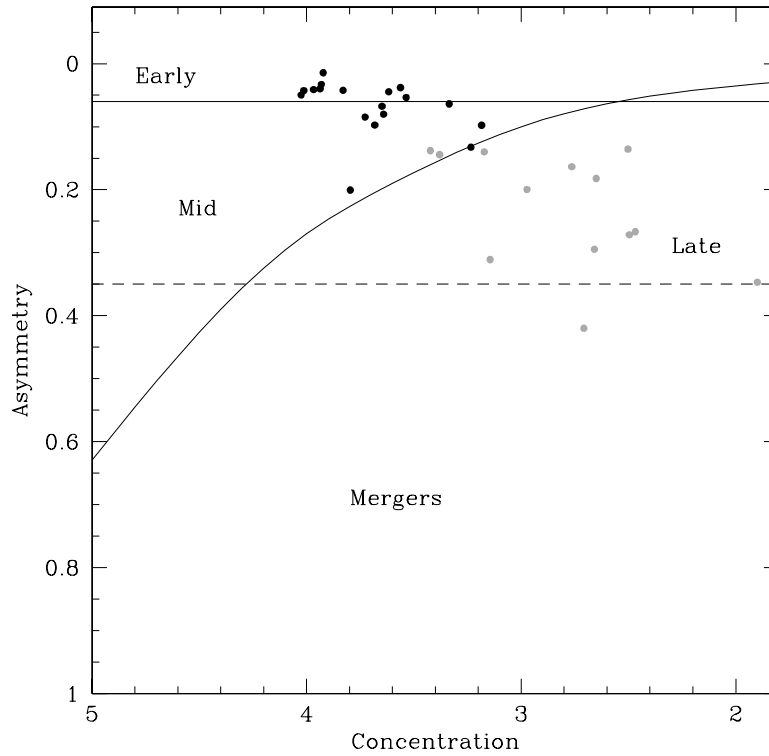


FIG. 1.—Asymmetry and Concentration values for the spectroscopically selected galaxies. The filled black circles represent our main sample of bona fide early-type galaxies. The distinction between early-, late-type, mid galaxies and mergers is from Conselice et al. (2004).

APPENDIX

errors on the measured isophotal parameters

When comparing the isophotal parameters of galaxies at different redshift and observed with different instruments, it becomes important to qualitatively establish the systematics in the data. For this reason, we simulated elliptical galaxies using a Sersic profile (Sersic 1968) with an index chosen between 3 and 4, an integrated magnitude and corresponding S/N ratio taken from the range spanned by the data. The input ellipticities and position angles were chosen among those measured for the bona fide early-type galaxies and the input a_3/a and a_4/a parameters were rigorously set to 0. The simulated galaxies were then convolved by the ACS PSF in the F775W filter; this PSF is the average image of stars in the UDF F775W frame.

We first ran ELLIPSE on the set of simulated galaxies convolved by the PSF and measured the isophotal parameters with the method described in Sect. 5. We then repeated the measurements on the simulated galaxies NOT convolved by the PSF. The results are summarized in Figures 35 and 36. When no PSF is applied, the output isophotal parameters agree extremely well with their respective input values, thus indicating that the S/N ratio of the data does not significantly affect our measurements (but see also Odewahn et al. 1997). The convolution with the PSF introduces deviations from the input parameters so that:

- i) the output ellipticities are underestimated by about 10% ;
 - ii) the output PA values are underestimated by about 3% ;
 - iii) the output a_3/a parameter is overestimated and measured to be about 0.2 at most;
 - iv) the output a_4/a parameter is also overestimated by an amount which increases with the input ellipticity. For $e < 0.5$ (the range in Table 2) we derive a discrepancy of +0.15 in a_4/a .
- These deviations do not show any correlation with the input magnitude and Sersic index and represent the systematic uncertainties on the values reported in Table 2.

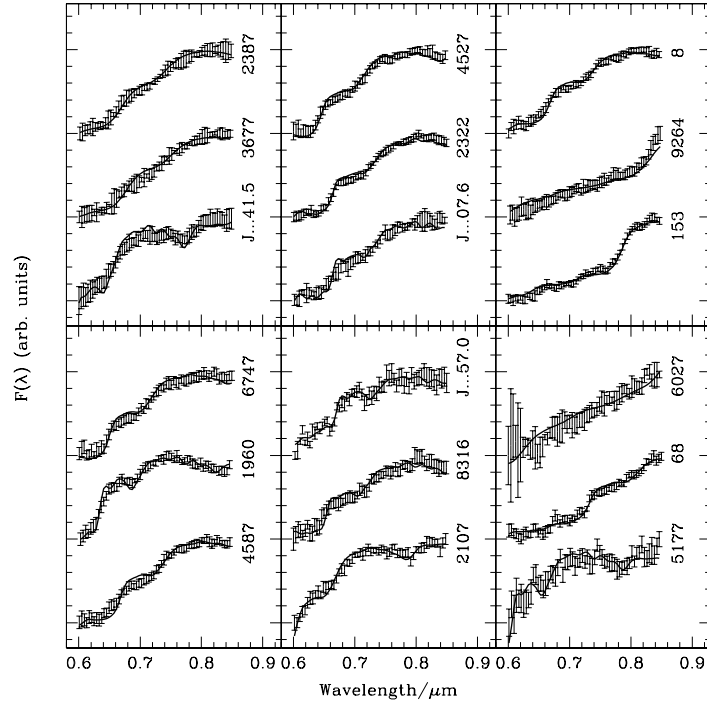


FIG. 2.— Spectral energy distributions of the 18 galaxies in our sample (see Table 1. Each one is labeled with the UDF numbers, except for those outside of UDF, for which we give part of the GOODS identification. The error bars are the observed ACS/G800L data and the lines are the best fits according to the CSP models (see text for details).

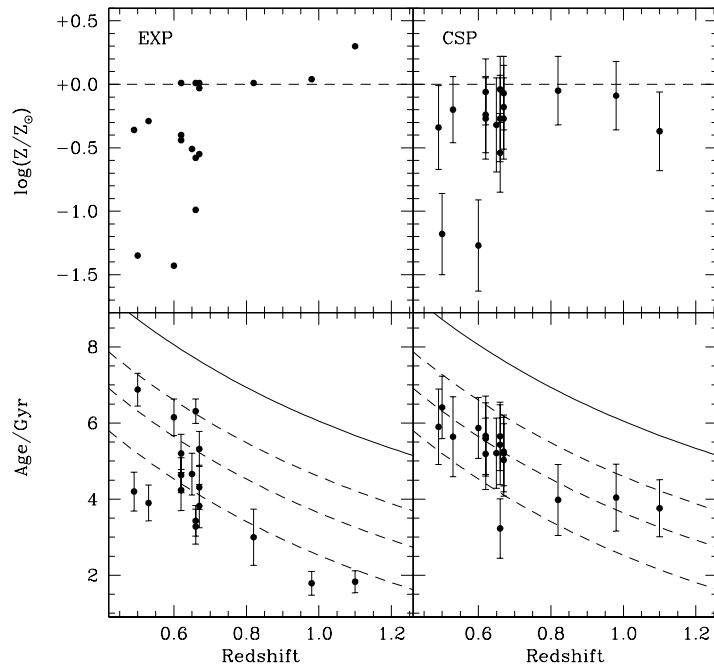


FIG. 3.— Age and metallicities corresponding to the best fit according to a simple exponentially decaying model (EXP; left) or a consistent chemical enrichment code (CSP; right). The dots are the average values of age or metallicity and the error bars represent the RM S of the distribution. Notice the EXP models assume a fixed metallicity for each star formation history. The solid lines in the bottom panel track the age of the Universe at a given redshift for a concordance cosmology. The dashed lines (from top to bottom) correspond to formation redshifts of $z_F = f5;3;2g$.

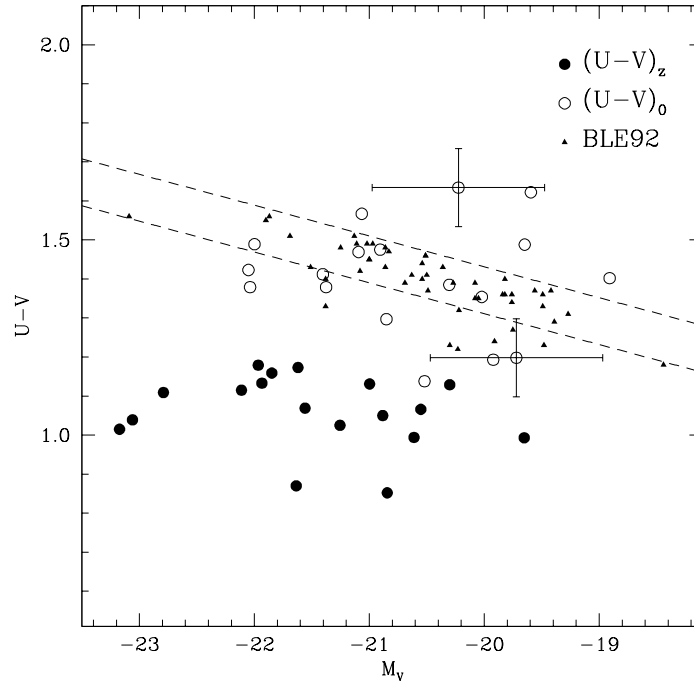


FIG. 4.—Restframe $U-V$ vs M_V color-magnitude relation. The filled dots correspond to our sample after a K -correction to restframe U and V passbands. The hollow circles are the $z = 0$ color-magnitude relation of the same sample. In order to evolve the stellar populations from their observed redshifts, we use the CSP model that gives the best fit. Typical error bars (including the effect of the K -correction) are shown. The triangles are Coma cluster galaxies from Bower et al. (1992) and the dashed lines delimit the best fit and scatter of this local cluster.

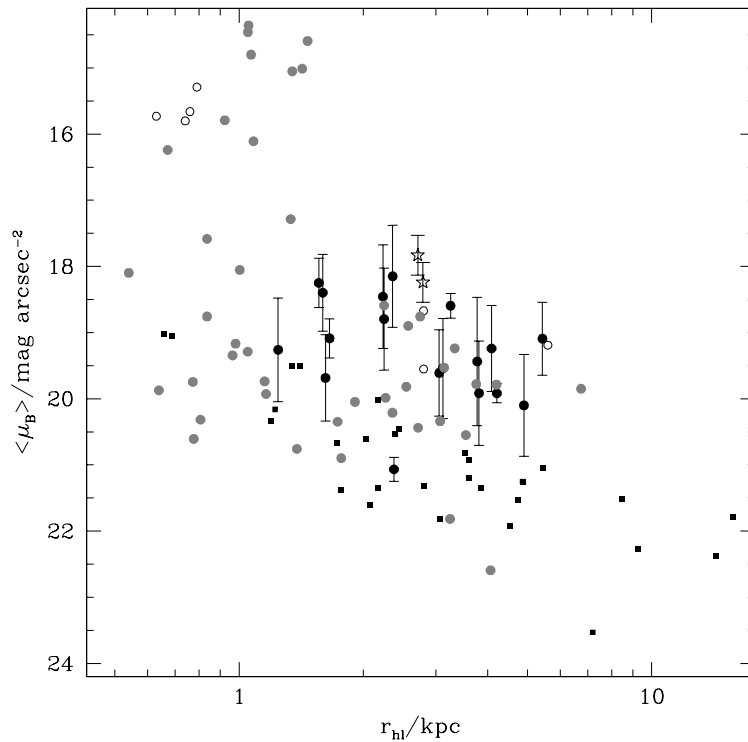


FIG. 5.—B-band Kormendy relation of our sample (black dots) compared to Coma cluster elliptical galaxies (squares; Jørgensen et al. 1995) and early-type galaxies from the HDF (grey dots; Fasano et al. 1998). The stars are the LBDS radio elliptical galaxies at $z = 1.5$ from Waddington et al. (2002), while the open dots represent the early-type galaxies at $z = 2$ studied by Daddi et al. (2005).

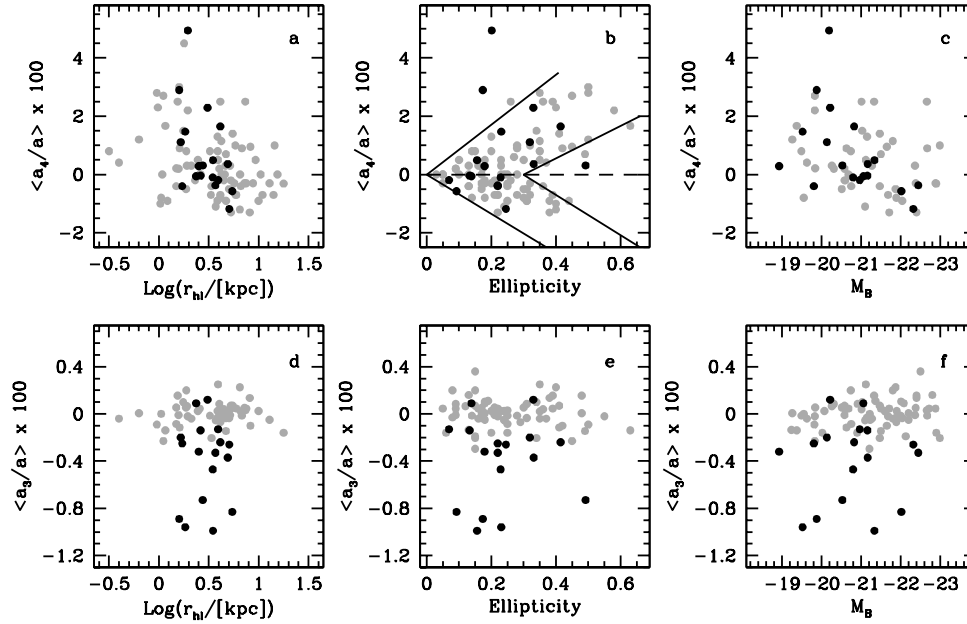


FIG. 6.—The corrected isophotal parameters of the bona fide early-type galaxies (black, filled circles) and of the nearby ellipticals studied by Bender et al. (1988, 1989, grey and filled circles). These parameters are also plotted as a function of the galaxy half-light radius r_{hl} and total absolute magnitude in restframe B band M_B . The solid lines in panel b highlight the region in ellipticity and a_4/a populated by nearby ellipticals.

The following Figures are available at <http://www.stsci.edu/science/grapes/papers/pasquali05>

FIG. 7.—Left-hand side panel: the $(V-I)$ color map of J033244.09-274541.5. Middle panel: a close-up of the central region ($1^{00}2 \ 1^{00}2$) in counts/s in the F775W filter. Right-hand side panel: the extinction map of the same region in units of magnitude.

FIG. 8.—The $(V-I)$ color maps of UDF 2322, UDF 4587, UDF 6027 and UDF 8316.

FIG. 9.—The $(V-I)$ color maps of UDF 9264, J033229.22-274707.6 and J033240.33-274957.0.

FIG. 10.—Left-hand side panel: the $(V-I)$ color map of UDF 2387. Middle panel: a close-up of the central region ($1^{00}2 \ 1^{00}3$) in counts/s in the F775W filter. Right-hand side panel: the extinction map of the same region in units of magnitude.

FIG. 11.—Left-hand side panel: the $(V-I)$ color map of UDF 3677. Middle panel: a close-up of the central region ($1^{00}3 \ 1^{00}3$) in counts/s in the F775W filter. Right-hand side panel: the extinction map of the same region in units of magnitude.

FIG. 12.—Left-hand side panel: the $(V-I)$ color map of UDF 4527. Middle panel: a close-up of the central region ($0^{00}8 \ 0^{00}7$) in counts/s in the F775W filter. Right-hand side panel: the extinction map of the same region in units of magnitude.

FIG. 13.—Left-hand side panel: the $(V-I)$ color map of UDF 6747. Middle panel: a close-up of the central region ($1^{00}1$

$1^{\text{h}}02^{\text{m}}$) in counts/s in the F775W filter. Right-hand side panel: the extinction map of the same region in units of magnitude.

FIG . 14.-The (V-I) color maps of UDF 8, UDF 68, UDF 1960 and UDF 2107.

FIG . 15.-Left-hand side panel: the (V-I) color map of UDF 153. Middle panel: a close-up of the central region ($1^{\text{h}}01^{\text{m}}1^{\text{s}}02^{\text{m}}$) in counts/s in the F775W filter. Right-hand side panel: the extinction map of the same region in units of magnitude.

FIG . 16.-Left-hand side panel: the (V-I) color map of UDF 5177. Middle panel: a close-up of the central region ($0^{\text{h}}09^{\text{m}}00^{\text{s}}.8$) in counts/s in the F775W filter. Right-hand side panel: the extinction map of the same region in units of magnitude.

FIG . 17.-The ELLIPSE parameters: surface brightness, ellipticity, PA, a_3 , a_4 as a function of distance from the center of J033229.22-274707.6 and derived in each of the F606W, F775W and F850LP filters.

FIG . 18.-As in Figure 17, but for UDF 2387. This galaxy has prominent dust lanes (cf. Figure 10).

FIG . 19.-As in Figure 17, but for UDF 1960. The spike at a distance of about $0^{\text{h}}04^{\text{m}}$ from the galaxy center is due to the presence of a blue clump (cf. Figure 14).

FIG . 20.-As in Figure 17, but for UDF 9264.

FIG . 21.-As in Figure 17, but for UDF 3677. This galaxy has prominent dust lanes (cf. Figure 11) which produce the spike in a_3/a at a distance of about $0^{\text{h}}02^{\text{m}}$ from the galaxy center.

FIG . 22.-As in Figure 17, but for UDF 8316.

FIG . 23.-As in Figure 17, but for UDF 6747. This galaxy has a remarkable disk substructure (cf. Figure 13).

FIG . 24.-As in Figure 17, but for UDF 68.

FIG . 25.-As in Figure 17, but for UDF 2322.

FIG . 26.-As in Figure 17, but for UDF 8. The increase in a_4/a at a distance of about $0^{\text{h}}08^{\text{m}}$ from the galaxy center is possibly due to the presence of a blue clump (cf. Figure 14).

FIG . 27.-As in Figure 17, but for UDF 6027. This early-type galaxy hosts a blue core (cf. Figure 8).

FIG . 28.-As in Figure 17, but for UDF153. This galaxy is surrounded by a faint and incomplete shell.

FIG . 29.-As in Figure 17, but for J033240.33-274957.0.

FIG . 30.-As in Figure 17, but for UDF4587.

FIG . 31.-As in Figure 17, but for UDF4527. This galaxy has a remarkable disk substructure (cf. Figure 12).

FIG . 32.-As in Figure 17, but for J033244.09-274541.5.

FIG . 33.-As in Figure 17, but for UDF2107.

FIG . 34.-As in Figure 17, but for UDF5177. This galaxy hosts a blue core (cf. Figure 16).

FIG . 35.-The comparison between the input and output ellipticities and PAs, for the simulated galaxies with (right-hand side panels) and without (left-hand side panels) convolution with the ACS PSF in the F775W .

FIG . 36.-The comparison between the input and output $h_{3=ai}$ and $h_{4=ai}$ for the simulated galaxies with (right-hand side panels) and without (left-hand side panels) convolution with the ACS PSF in the F775W .